NASA/TM—2003-212017 AIAA–2003–0652

Design-of-Experiments to Reduce Life-Cycle Costs in Combat Aircraft Inlets

Bernhard H. Anderson
Glenn Research Center, Cleveland, Ohio

Henry D. Baust
Wright Patterson Air Force Base, Dayton, Ohio

Johan Agrell
Swedish Defence Research Agency, Bromma, Sweden

January 2003

The NASA STI Program Office . . . in Profile

Since its founding, NASA has been dedicated to the advancement of aeronautics and space science. The NASA Scientific and Technical Information (STI) Program Office plays a key part in helping NASA maintain this important role.

The NASA STI Program Office is operated by Langley Research Center, the Lead Center for NASA's scientific and technical information. The NASA STI Program Office provides access to the NASA STI Database, the largest collection of aeronautical and space science STI in the world. The Program Office is also NASA's institutional mechanism for disseminating the results of its research and development activities. These results are published by NASA in the NASA STI Report Series, which includes the following report types:

- TECHNICAL PUBLICATION. Reports of completed research or a major significant phase of research that present the results of NASA programs and include extensive data or theoretical analysis. Includes compilations of significant scientific and technical data and information deemed to be of continuing reference value. NASA's counterpart of peer-reviewed formal professional papers but has less stringent limitations on manuscript length and extent of graphic presentations.

- TECHNICAL MEMORANDUM. Scientific and technical findings that are preliminary or of specialized interest, e.g., quick release reports, working papers, and bibliographies that contain minimal annotation. Does not contain extensive analysis.

- CONTRACTOR REPORT. Scientific and technical findings by NASA-sponsored contractors and grantees.

- CONFERENCE PUBLICATION. Collected papers from scientific and technical conferences, symposia, seminars, or other meetings sponsored or cosponsored by NASA.

- SPECIAL PUBLICATION. Scientific, technical, or historical information from NASA programs, projects, and missions, often concerned with subjects having substantial public interest.

- TECHNICAL TRANSLATION. English-language translations of foreign scientific and technical material pertinent to NASA's mission.

Specialized services that complement the STI Program Office's diverse offerings include creating custom thesauri, building customized databases, organizing and publishing research results . . . even providing videos.

For more information about the NASA STI Program Office, see the following:

- Access the NASA STI Program Home Page at ***http://www.sti.nasa.gov***

- E-mail your question via the Internet to help@sti.nasa.gov

- Fax your question to the NASA Access Help Desk at 301–621–0134

- Telephone the NASA Access Help Desk at 301–621–0390

- Write to:
  NASA Access Help Desk
  NASA Center for AeroSpace Information
  7121 Standard Drive
  Hanover, MD 21076

NASA/TM—2003-212017 AIAA–2003–0652

Design-of-Experiments to Reduce Life-Cycle Costs in Combat Aircraft Inlets

Bernhard H. Anderson
Glenn Research Center, Cleveland, Ohio

Henry D. Baust
Wright Patterson Air Force Base, Dayton, Ohio

Johan Agrell
Swedish Defence Research Agency, Bromma, Sweden

Prepared for the
41st Aerospace Sciences Meeting and Exhibit
sponsored by the American Institute of Aeronautics and Astronautics
Reno, Nevada, January 6–9, 2003

National Aeronautics and
Space Administration

Glenn Research Center

January 2003

The Aerospace Propulsion and Power Program at
NASA Glenn Research Center sponsored this work.

Available from

NASA Center for Aerospace Information
7121 Standard Drive
Hanover, MD 21076

National Technical Information Service
5285 Port Royal Road
Springfield, VA 22100

Available electronically at http://gltrs.grc.nasa.gov

DESIGN-OF-EXPERIMENTS TO REDUCE LIFE-CYCLE COSTS IN COMBAT AIRCRAFT INLETS

Bernhard H. Anderson
National Aeronautics and Space Administration
Glenn Research Center
Cleveland, Ohio 44135

Henry D. Baust
Wright Patterson Air Force Base
Dayton, Ohio 45433

Johan Agrell
Swedish Defence Research Agency
Bromma, Sweden

ABSTRACT

It is the purpose of this study to demonstrate the viability and economy of *Design-of-Experiments* (DOE) to arrive at micro-secondary flow control installation designs that achieve optimal inlet performance for different mission strategies. These statistical design concepts were used to investigate the properties of "low unit strength" micro-effector installation. "Low unit strength" micro-effectors are micro-vanes, set a very low angle-of-incidence, with very long chord lengths. They are designed to influence the near wall inlet flow over an extended streamwise distance. In this study, however, the long chord lengths were replicated by a series of short chord length effectors arranged in series over multiple bands of effectors. In order to properly evaluate the performance differences between the single band extended chord length installation designs and the segmented multi-band short chord length designs, both sets of installations must be optimal. Critical to achieving optimal micro-secondary flow control installation designs is the understanding of the factor interactions that occur between the multiple bands of micro-scale vane effectors. These factor interactions are best understood and brought together in an optimal manner through a structured DOE process, or more specifically *Response Surface Methods* (RSM).

INTRODUCTION

The current development strategy for combat air-vehicles is directed towards reduction in the Life-Cycle Cost (LCC) with little or no compromise to air-vehicle performance and survivability. This strategy has been extended to the aircraft component level, in particular, the inlet engine diffuser system. One method to reduce inlet system LCC is to reduce its structural weight and volume. Consequently, advanced compact air vehicle inlet configurations are being made more compact (or shorter) to achieve weight and volume (and LCC) reduction. However, compact S-duct diffusers (see Figures (1) and (2)) are characterized by high distortion and low pressure recovery, which are produced by extreme wall curvature and strong secondary flow gradients. These characteristics are further aggravated by maneuvering conditions. Since survivability rather than aerodynamic performance often drives the inlet design, it is expected that the flow quality entering the turbine engine will present an additional challenging environment for both fan/compressor surge margin and aeromechanical vibration. Interest in High Cycle Fatigue (HCF) research by the US aerospace community has been spurred by discrepancies between the expected durability of engine components compared to that actually experienced in the field. Recognizing that inlet distortion is a forcing function for vibration in the fan components, methods for increasing HCF Life Expectancy can been combined with techniques for inlet recovery and engine face distortion management. Therefore, to enable acceptable performance levels in such advanced, compact inlet diffuser configurations, micro-scale secondary flow control (MSFC) methods are being developed to manage the recovery, distortion, and HCF aspects of distortion.[(1)-(2)]

One of the most difficult tasks in the design of a MSFC installation for optimal inlet operation is arriving at the geometric placement, arrangement, number, size and orientation of the effector devices within the inlet duct to achieve optimal performance.These effector devices can be either mechanical or fluidic.This task is complicated not only by the large number of possible design variables available to the aerodynamicist, but also by the number of decision parameters that are brought into the design process. By including the HCF effects in the inlet design process, the aerodynamicist has a total of seven individual response variables that measure various aspects of inlet performance. These include the inlet total pressure recovery, the inlet total pressure recovery distortion at the engine face and the first five Fourier harmonic 1/2-amplitudes contained in the engine face distortion pattern. Each of these responses must be maximized, minimized, constrained or unconstrained while searching for the optimal combination of primary design variable values that satisfy the mission requirements. Numerical optimization procedures that have been successful with some aerodynamic problems give little assistance to the design of micro-scale secondary flow installations. It is very difficult to incorporate large numbers of independent factor and response variables into such procedures. Further, they are very expensive to use if the individual CFD experiments are solutions to the full Navier-Stokes equations in three dimensions.However, there is a statistical approach to the problem which combines an optimally sequenced pattern of Design-of-Experiments (DOE), statistical model building, and system optimization called *Response Surface Methods* (RSM).

In this research study on MSFC for compact inlet diffusers, three objectives were considered important, namely: (1) to determine the design characteristics of micro-scale secondary flow control configurations, (2) to evaluate the ability of MSFC to manage the aeromechanical effects of engine face distortion, and (3) to evaluate the effectiveness

of robust methodologies to design fixed "open loop" MSFC installation designs in comparison to adaptive "closed loop" designs which would require a control system. Anderson and Keller[3] covers the first two research objectives while Anderson and Keller[4]-[5] covers the third objective and describes a robust design methodology whereby the hard-to-control mission variables can be explicitly included in the design of optimal MSFC installations. A forth report in this series by Anderson and Keller[6] evaluates the impact of engine face rake geometry (i.e. number of rake arms) and its use (i.e. with and without clocking), on the random and systematic measurement errors associated with estimating the first five Fourier harmonic 1/2-amplitudes of engine face distortion. It was concluded in Anderson and Keller[4]-[5] that micro-scale secondary flow control using multi-bands of micro-vane effectors were inherently robust, provided the installations was optimally designed. Robustness in this situation means that it is possible to design fixed MSFC robust installations (i.e. open loop) which operates well over the range of mission variables and is only marginally different from adaptive (i.e. closed loop) installation designs which would require a control system. However, this improvement in engine face distortion came at the expense of total pressure recovery. In order to overcome the high loss associated with "high unit strength" micro-vane effectors, the micro-vane angle of incidence was greatly reduced while compensating for loss of unit strength by increasing the length of the micro-vane effector units. These devices, called "low unit strength" micro-vane effectors, demonstrated excellent robustness properties over the range of mission variables. "Low unit strength" micro-vane effectors also demonstrated substantial improvement in inlet total pressure recovery over "high unit strength" micro-vane effectors, Anderson, Baust, and Agrell.[6] Therefore effective inlet flow control management of engine face distortion was achieved by reducing the unit strength of the vane effector and allowing the installation design to influence the inlet flow over a longer streamwise distance.

In this study, however, the long chord lengths were replicated by a series of short chord length effectors arranged in series over multiple bands of effectors. Thus, it is the purpose of this study to perform a comparative examination between the single band extended chord length installations of Anderson, Baust, and Agrell,[6] with the installation made up of multiple bands of short chord length "low unit strength" micro-effectors extending over approximately the same streamwise distance. In order to properly evaluate the performances difference between the single band extended chord length installation designs and the segmented multi-band short chord length designs, both sets of installations must be optimal. Critical to achieving optimal micro-secondary flow control installation designs is the understanding of the factor interactions that occur between the multiple bands of micro-scale vane effectors. These factor interactions are best understood and brought together in an optimal manner through a structured Design-of-Experiments process, or more specifically *Response Surface Methods* (RSM).

NOMENCLATURE

AIP	Aerodynamic Interface Plane
c	Effector Chord Length
CCF	Central Composite Face-Centered
CFD	Computational Fluid Dynamics
D	Engine Face Diameter
DC60	Circumferential Distortion Descriptor
DOE	Design of Experiments
h	Effector Blade Height
HCF	High Cycle Fatigue
Fk/2	k^{th} Fourier Harmonic 1/2-Amplitude
FM/2	Mean Fourier Harmonic 1/2-Amplitude
L	Inlet Diffuser Length
LCC	Life Cycle Costs
MSFC	Micro-Scale Secondary Flow Control
Mt	Inlet Throat Mach Number
n	Number of Effector Vanes per Band
PFAVE	Average Inlet Total Pressure at AIP
PAVCRIT	Minimum Total Pressure over Angle
QAVE	Average Dynamic Pressure at AIP
R	Inlet Radius
R_{cl}	Centerline Radius
R_{ef}	Engine Face Radius
R_{thr}	Inlet Throat Radius
Re	Reynold Number per ft.
RSM	Response Surface Methodology
S	Standard Deviation
S_{clock}	Standard Deviation over the Clocking Angles
UAV	Unmanned Air Vehicle
UCAV	Unmanned Combact Air Vehicle
X_{cl}	Axial Distance Along the Duct Centerline
Y_A	Upper 95% Confidence Interval
Y_{CFD}	Response Predicted by CFD Analysis
Y_{DOE}	Response Predicted by DOE Analysis
Z_{cl}	Centerline Offset Displacement
α	Inlet Angle-of-Incidence
β	Effector Vane Angle-of-Incidence
ΔZ_{cl}	Inlet Centerline Offset
γ	Inlet Angle-of-Yaw

RESULTS AND DISCUSSION

Baseline Flow in the Redesigned M2129 Inlet S-Duct

The redesigned M2129 inlet S-duct used in this study was considered similar to the original DERA/M2129 inlet S-duct defined by AGARD FDP Working Group 13 Test Case 3,[7] using Lip No. 3 and Forward Extension No. 2. This inlet design was first proposed by Willmer, Smith and Goldsmith,[8] and has been used extensively in the US and UK to explore inlet flow control installation design. The centerline for the redesigned M2129 inlet is given by the equation

$$Z_{cl} = -\Delta Z_{cl}\left(1 - \cos\left(\pi \cdot \frac{X_{cl}}{L}\right)\right) \qquad (1)$$

while the radius distribution measured normal to the inlet center-line is given by the expression

$$\left(\frac{R_{cl} - R_{thr}}{R_{ef} - R_{thr}}\right) = 3\left(1 - \frac{X_{cl}}{L}\right)^4 - 4\left(1 - \frac{X_{cl}}{L}\right)^3 + 1 \qquad (2)$$

where $R_{thr} = 2.5355$ inches, $R_{ef} = 3.0$ inches, $L = 15.0$ inches, and $\Delta Z_{cl} = 5.401$ inches. The redesign of the M2129 inlet was such that the new inlet matches the static pressure gradients normally found in typical UAV or UCAV designs. Therefore, the new inlet is more compact than the original M2129 inlet S-duct. As a consequence, supersonic flow will

develop in this inlet when the inlet throat Mach number increases much above 0.70. The geometry and grid structure for the resigned M2129 inlet S-duct is described in detail in Anderson, Baust, and Agrell.[6].

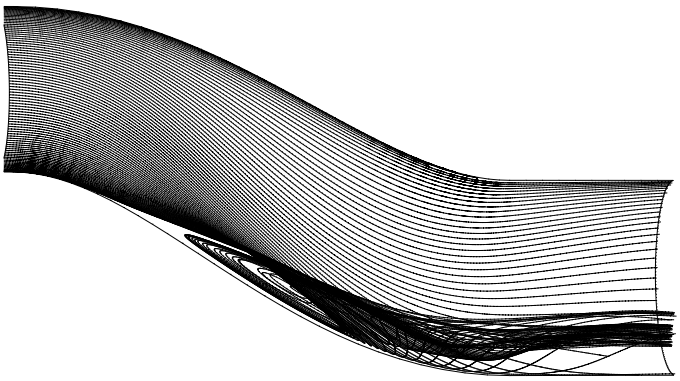

Figure (1): Near wall streamlines in baseline inlet S-duct

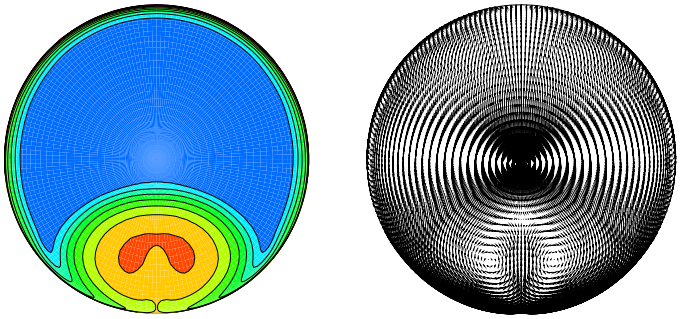

(a) Pressure Recovery **(b) Velocity Vectors**

Figure (2): Engine face flow field in baseline inlet S-duct.

Traditionally, this type of compact inlet duct would be excluded from design consideration since it is characterized by severe wall curvature that induces strong secondary flows. These strong secondary flow can cause a flow separation called vortex lift-off. See Figure (1). This type of 3D flow separation results in severe total pressure losses and engine face distortion. Figure (2) presents the engine face total pressure recovery contours and secondary flow velocity vectors for the redesigned DERA/M2129 inlet S-duct at a throat Mach number of 0.70. A vortex pair is dominant in the engine face flow field and this was accompanied by very severe engine face total pressure distortion.

Inlet Flow Control Design Approach

In the secondary flow control concept, micro-scale actuation is used as an approach called "secondary flow control" to alter the inlet S-duct inherent secondary flow with the goal of simultaneously improving the critical system level performance metrics of total pressure recovery, engine face distortion, and HCF characteristics. In studying the influence of micro-vane chord length[1] on inlet performance, it was determined that this factor was very important parameter in reducing engine face distortion as well as managing the harmonic content of engine face distortion. While there appear to be limits on the total number and strength of the individual effector units[1] in managing engine face distortion, there appear to be no such limits on micro-vane chord length. By installing multiple bands of micro-effector units, the chord length can be effectively increased,[5] and engine face distortion managed. However, this improvement in engine face distortion came at the expense of total pressure recovery. In order to overcome the dimensional limit of chord length, the micro-vane angle of incidence can be greatly reduced while compensating by increasing the length of the micro-vane effector units. Hence effective inlet flow control management of engine face distortion can be achieved by reducing the unit strength of the vane effector and allowing the installation design to influence the inlet flow over an extended streamwise distance. With this combination, the total pressure losses associated with micro-vane effectors become very small, and a large overall performance gain achieved.[6] In this study, however, the extended chord lengths were replicated by a series of short chord length effectors arranged in series over multiple bands of effectors. If discrete micro-vane effectors arranged in multiple bands perform in a similar manner as extended chord length single band effectors,[6] the possible opens that multiple bands of "low unit strength" discrete micro-jets will also perform well. In other words, the effectiveness of "low unit strength" micro-jets may be substantially improved by multi-band arrangements.

Inlet Flow Control Installation Design

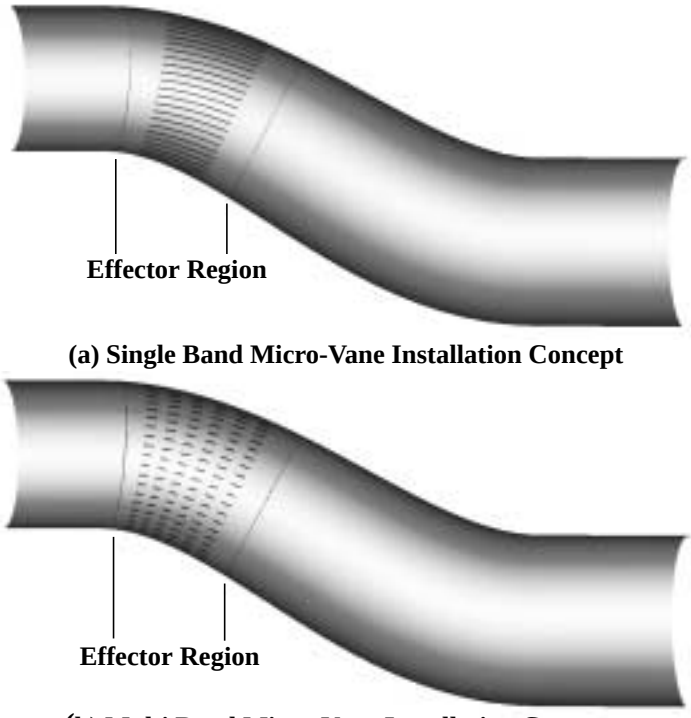

(a) Single Band Micro-Vane Installation Concept

(b) Multi Band Micro-Vane Installation Concept

Figure (3): Location of effector region within inlet S-duct configurations.

To manage the flow in the redesigned M2129 inlet S-duct, an installation arrangement of micro-scale effectors was placed in the upstream section near the inlet throat. See Figure (3). For the single band installation, the micro-effectors extend

over a streamwise distance of about 72.0 mm., Figure (3a). The multi band installation extended over the nominally the same streamwise distance, but was segmented into a six band arrangement of micro effectors. See Figure (3b).The chord length of individual multi-band installation effectors was about 8.0 mm., while the streamwise spacing between the micro-effectors was nominally 6.0 mm. These micro-scale effectors were micro-vanes, the largest height being about the average height of the momentum layer just downstream of the inlet throat or about 2.0 mm. The purpose of these micro-vanes was to create a set of co-rotating vortices that will quickly merge to form a thin layer of secondary flow that will counter the formation of the passage vortex pair.

Factor	Range
Number of Micro-Vane Effectors per Band, n	13 to 27
Micro-Vane Angle-of-Incidence (degs), β	0.0 to 8.0
Micro-Vane Effector Height (mm), h	1.0 to 2.0

Table (1): Factor variables which establish the DOE design.

Variable	Value
Micro-Vane Effector Thickness (mm), t	0.138
Micro-Vane Effector Chord Length (mm), c	8.0
Nominal Streamwise Chord Spacing (mm), Δc	6.0
Inlet Total Pressure (lbs/ft^2), Pt	10506.0
Inlet Total Temperature (^{o}R), Tt	517.0
Inlet Throat Mach Number, Mt	0.70
Inlet Angle-of-Incidence (degs.), α	0.0
Inlet Angle-of-Yaw (degs), γ	0.0

Table (2): Variables held constant.

The DOE approach for the multi-band installation study followed directly from the objectives previously stated and was reflected in the layout of the design factors listed in Table (1). The factor variables were the number of vane effector units per band (n), the micro-vane angle-of-incidence (β) and the micro-vane effector height (h). Table (2) shows the variables that were held constant during this study. They included the thickness of the micro-vanes (t), the micro-vane chord length (c), the nominal streamwise spacing between individual micro-effectors (Δc), the inlet operating total pressure (Pt) and temperature (Tt), angle-of incidence (α), and the inlet angle-of-yaw (γ). Table (3) displays the response variables for this study. They include the inlet total pressure recovery (PFAVE), the engine face distortion (DC60), and the first five Fourier harmonic 1/2-amplitudes of engine face distortion (F1/2, F2/2, F3/2, F4/2, and F5/2).

Response	Nomenclature
Engine Face Total Pressure Recovery	PFAVE
Engine Face Distortion	DC60
1st Fourier Harmonic 1/2-Amplitude	F1/2
2nd Fourier Harmonic 1/2-Amplitude	F2/2
3rd Fourier Harmonic 1/2-Amplitude	F3/2
4th Fourier Harmonic 1/2-Amplitude	F4/2
5th Fourier Harmonic 1/2-Amplitude	F5/2

Table (3): DOE response variables.

The DOE strategy selected was a Central Composite Face-Centered (CCF) DOE. This strategy resulted in 15 unique CFD experimental cases that are shown in Table (4). Notice that these DOE cases covered a wide range of installation geometries. This particular DOE, like most DOE strategies, varied more than one factor at a time. Further, this layout of 15 cases permitted the estimation of both linear and curvilinear effects as well as two-factor interactive or synergistic effects among the DOE factors.

Config.	n	β	h
nvg901	13	0.0	1.0
nvg902	27	0.0	1.0
nvg903	13	8.0	1.0
nvg904	27	8.0	1.0
nvg905	13	0.0	2.0
nvg906	27	0.0	2.0
nvg907	13	8.0	2.0
nvg908	27	8.0	2.0
nvg909	13	4.0	1.5
nvg910	27	4.0	1.5
nvg911	20	0.0	1.5
nvg912	20	8.0	1.5
nvg913	20	4.0	1.0
nvg914	20	4.0	2.0
nvg915	20	4.0	1.5

Table (4): Central Composite Face-Centered (CCF) DOE design

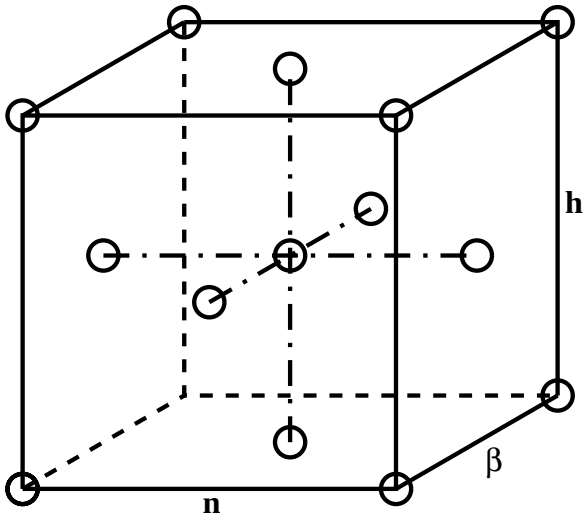

Figure (4): Graphical representation of the Central Composite Face-Centered (CCF) DOE design.

A graphical representation of the Central Composite Face-Centered DOE used in the multi-band installation study is presented in Figure (4). The DOE cases are represented in this figure by the circular symbols, where the symbol locations on the cube signify its factor value. This DOE is called a composite DOE because the organization of cases is composed of a factorial part and a quadratic part. The factorial part of the DOE is composed of 2^3 possible cases, i.e. 8 possible factorial cases, which are represented by the eight corner locations of the cube in Figure (4). The remaining cases in Figure (4) are the quadratic part of the DOE. The quadratic cases allow for the evaluation of the curvilinear effects. All together, there are a total of 15 cases in a Central Composite Face-Centered DOE with three factor variables. Notice the balanced layout of cases in Figure (4). This layout of cases represents the smallest number of CCF DOE cases that allows for the evaluation of linear and curvilinear effects as well as all two-factor interactive or synergistic effects.

Each of the 15 cases in Table (4) were run with a Reynolds-averaged Navier-Stokes code[11] that allowed for numerical simulation of micro-vane effectors without the need to physically embed the vane effectors within the CFD grid structure. However, for the present study the individual vanes were incorporated into the half cylindrical grid structure These micro-vanes had a thickness of 0.138 mm. See Table (2). The computational grid surrounding each micro-vane effector in the installation was developed such that it reasonably resolved the boundary layer development on both the suction and pressure surfaces. Because wall functions were used in the calculations, the grid resolution for the individual micro-vanes was simplified. The boundary layer along the micro-vane edges was assumed to be negligible, and therefore not resolved in the computational grid. The half cylindrical grid structure was composed of three blocks: an upstream block, an effector section containing the micro-vanes, and a downstream block. See Figures (3b) and (4b). The computational half-plane grid varied in total number of mesh points from about 950,000 to 1,150,000 depending on the micro-vane configuration. All CFD calculations were accomplished assuming half cylindrical symmetry. A two-equation k-l turbulence model was used in this study. The model consists of transport equation for the turbulent kinetic energy and turbulent length scale. The model includes a near-wall model and compressible corrections for high speed flows.

Harmonic Analysis of Distortion

The overall methodology used to obtain the harmonic content of inlet distortion is described in great detail in Anderson, Baust, and Agrell,[6] and in Anderson and Keller.[7] This methodology is characterized by the use of radial weighting factors applied to the total pressure rake measurements. These radial weighting factors compress the rake information to a single radius ring of data samples, where the number of data samples corresponds to the number of arms of the measurement rake. As a result of that accuracy study in estimating the Fourier harmonic 1/2-amplitudes from an engine face rake,[7] the rake and methodology chosen for this study was the 80-probe clocked rake because it provided the lowest error in estimating the first five Fourier harmonic 1/2-amplitudes of engine face distortion. Clocking the AIP rake means that N separate measurements were taken, and at each measurement, the angular orientation of the rake was advanced an by an amount 1/N time the rake angle.The rake angle is the ratio of 360^o divided by the number of arms in the AIP rake. For example, a standard 80-probe rake has 16-arms. Hence the rake angle is 22.5^o. Therefore total pressure measurements were obtained at each 22.5^o/N angular position of the rake. The span-weighted average total pressure was calculated for the 80-probe rake by multiplying the probe total pressure by the span-weighted coefficients, and adding the results over the five probes of the rakes to form a single radius ring of data samples.

Since the rake at the engine face was “clocked”, a complete set of “repeats” was generated at each experimental run in Table (4). From the engine face patterns at each of the 10 clocking angles, a Fourier analysis was performed on the sample set of data and a standard deviation of the “repeats”, S_{clock}, was determined for each of the Fourier harmonic 1/2-amplitudes. In order to check the constant variance assumption associated with least square regression, a simple F-test for comparing the minimum standard deviation to the maximum standard deviation ($F = S^2_{max}/S^2_{min}$) was conducted for each of the five responses. The results indicated that the F-test exceeded the 95% confidence critical value of $F(0.975,9,9) = 4.03$. Hence, the assumption of constant variance across the design space had to be discarded. This meant that a regression technique known as weighted least squares regression had to be employed for analyzing the 10 x 15 = 150 data samples in the DOE. The weights in these regression analyses were set to $1/S^2_{clock}$.

The data reduction for the inlet total pressure recovery and engine face distortion differed greatly from the harmonic analysis of distortion described. There exists no recognized methodology to evaluate the Fourier harmonic 1/2-amplitudes of engine face distortion for more than five probes in the radial direction. Hence, evaluating the Fourier harmonic 1/2-amplitude directly from the computational mesh had to be discarded. However, both the inlet total pressure recovery and engine face distortion can and were calculated directly from the computational grid at the engine face station. This computational mesh was composed of 49 x 121 grid points in the full-plane. The DC60 engine

face distortion descriptor is defined such that it can be determined from either a computational grid or a standard measurement rake. It is the only recognized distortion descriptor that has this property, and hence, was chosen for this study. The DC60 engine face distortion descriptor is a measure of the difference between the engine face or AIP average total pressure (PFAVE) and the lowest average total pressure in any sector defined by a critical angle of 60^o (PAVCRIT), divided by the average dynamic pressure at the engine (AIP) face. Hence

$$DC60 = \frac{(PFAVE - PAVCRIT)}{QAVE} \quad (3)$$

Response Surface Solutions and Factor Interactions

Presented in Figures (6) through (8) is the two way statistical factor interactions (n*β) between the micro-vane effector bands. Comparisons are made in each figure for the inlet total pressure recovery (PFAVE), engine face distortion (DC60) characteristics, and the mean of the first five Fourier harmonic 1/2-amplitudes (FM/2) of distortion. A statistical interaction exists between two independent factor variables X1 and X2 when the effect of X1 on response Yi is affected by the value of X2. In other words, the effect of factor X1 on response Yi is not unique, but changes as a function factor X2.

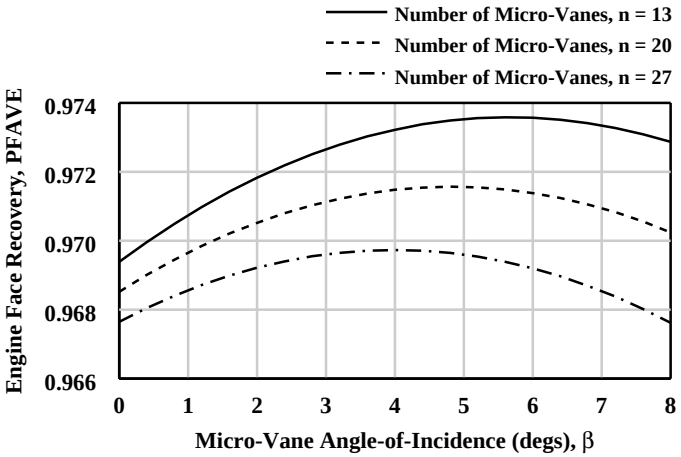

Figure (6): Effect of micro-vane number (n) and angle-of incidence (β) on engine face total pressure recovery (PFAVE), h = 2.0 (mm).

For example, Figures (6) through (8) presents the inlet performance metrics PFAVE, DC60 and FM/2 as a function the micro-vane angle-of-incidence (β) at three levels of number of vane-effectors per band (n). A particularly strong (n*β) factor interaction exist for the inlet total pressure recovery (PFAVE) response surface, which can be seen in Figure (6). As the number of micro-vane effectors per band (n) decreases from 27 to 13, there is a dramatic increase in total pressure recovery (PFAVE), and this improvement in recovery is very different at an effector angle-of-incidence of 0.0^o as compared to 8.0^o. In other words, the effect of micro-vane effector angle-of-incidence (β) of (PFAVE) changes as the number of micro-vane effectors per band (n) decreases. With 27 micro-vane effectors per band, the optimal micro-vane angle-of-incidence setting is 4.0^o, while for 13 micro-vane effectors per band, the optimal angle-of-incidence setting is 5.5^o. Likewise, (n*β) interactions exist for engine face distortion (DC60) response, Figure (7), and the mean of the first five components of the Fourier harmonic 1/2-amplitudes of distortion (FM/2), Figure (8), These (n*β) indurations effect the response surfaces for (DC60) and (FM/2) in varying degrees.

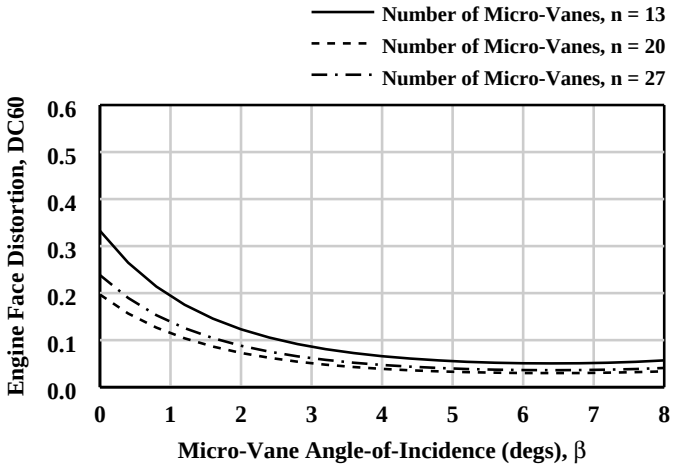

Figure (7): Effect of micro-vane number (n) and angle-of incidence (β) on engine face distortion (DC60), h = 2.0 (mm).

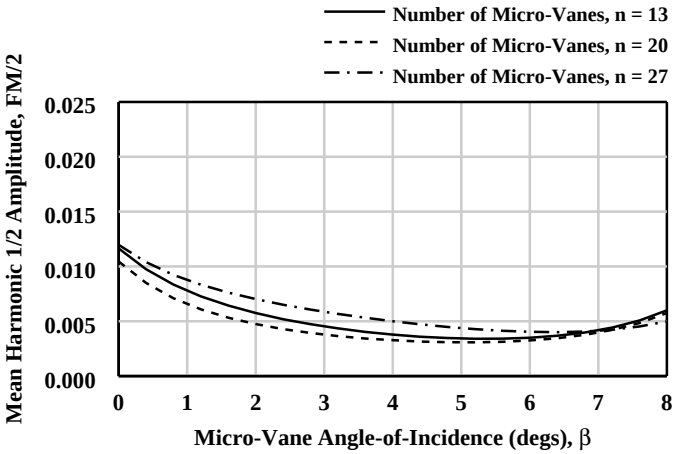

Figure (8): Effect of micro-vane number (n) and angle-of incidence (β) mean Fourier harmonic 1/2-amplitude (FM/2), h = 2.0 (mm)

In general, it is quite remarkable that very small angles-of-incidences are required to achieve large improvements in performance using multiple bands of short chord length micro-effectors. When the angle-of-incidence is set to 0^o, the micro-vanes act as fences and perform very poorly. With very small angle-of-incidences, large increases in total pressure recovery (PFAVE) were achieved, and substantial decreases in DC60 engine face distortion and the mean Fourier harmonics 1/2-amplitudes (FM/2) were realized. See Figures (6), through (8).

Optimal Flow Control Installations Designs

To illustrate the potential of RSM to design and optimize MSFC installations, three mission strategies were considered for the subject inlet, namely (1) Maximum Performance, (2) Maximum Engine Stability mission, and (3) Maximum HCF Life Expectancy. The Maximum Performance mission minimized the inlet total pressure losses, the Maximum Engine Stability mission minimized the engine face distortion, while the Maximum HCF Life Expectancy mission minimized the mean of the first five Fourier harmonic amplitudes, i.e. "collectively" reduced all the harmonic 1/2-amplitudes of engine face distortion. Each of the mission strategies was subject to a low engine face distortion constraint, i.e. DC60 ≤ 0.10, which is a level acceptable for commercial engines, and a constraint on each individual Fourier harmonic amplitudes of Fk/2 ≤ 0.015, k = 1 to 5.

Maximum Performance Mission - To obtain the optimal Maximum Performance installation design, a search was made over the factor variable space to find that installation that minimized the inlet duct losses

$$Y = (1 - PFAVE) \tag{3}$$

This search was subject to the engine face distortion constraint that

$$DC60 \le 0.10 \tag{4}$$

while the individual Fourier harmonic 1/2 amplitudes of distortion were each constrained to

$$\frac{Fk}{2} \le 0.015 \tag{5}$$

where k = 1 to 5. The resulting optimal values of the DOE factors were n =13, $\beta = 5.6^{o}$, and h = 2.0 mm.

Maximum Engine Stability Mission - To obtain the optimal Maximum Engine Stability installation designs, a search was made over the factor variable space to locate that installation geometry that minimized the decision parameter:

$$Y = (DC60) \tag{6}$$

subject to inlet total pressure recovery (PFAVE) being unconstrained, while the constraint on each Fourier harmonic 1/2 amplitude of distortion satisfy the relationship:

$$\frac{Fk}{2} \le 0.015 \tag{7}$$

where k = 1 to 5. The resulting optimal values of the DOE factors were n =13, $\beta = 5.6^{o}$, and h = 2.0 mm.

Maximum HCF Life Expectancy Mission -The optimal Maximum HCF Life Expectancy MSFC installation was determined through a search process over the factor variable space to locate that installation geometry that minimized the mean of the first five Fourier harmonic 1/2 amplitudes of distortion, i.e

$$Y = \frac{1}{5}\sum_{k=1}^{5}\left(\frac{Fk}{2}\right) \tag{8}$$

This search was subject to the inlet total pressure recovery (PFAVE) being unconstrained and the following constraint on the engine face distortion:

$$DC60 \le 0.01 \tag{9}$$

and constraint on the individual Fourier harmonic 1/2 amplitudes of distortion:

$$\frac{Fk}{2} \le 0.015 \tag{10}$$

where k = 1 to 5. The resulting optimal values of the DOE factors were n =13, $\beta = 5.6^{o}$, and h = 2.0 mm.

CFD Validation Test Cases - In order to validate the DOE prediction for the optimal Maximum Performance, Maximum Engine Stability, and Maximum HCF Life Expectancy installation designs, a set of three cases were run using the optimal factor values determined from the search procedure described. Each of the three CFD cases were run with a Reynolds-averaged Navier-Stokes code, and the performance results were tabulated in Table (5). The engine face total pressure recovery contours for the three CFD validation cases are presented in Figure (9). Again, the circumferential uniform nature of the engine face distortion patterns for the three optimal installation designs can clearly be seen in Figure (9).

Factor/ Response	Max. Perf.	Max. Stability	Max. HCF Life
n	13	22	19
β	5.6	6.4	5.2
h	2.0	2.0	1.70
PFAVE	0.97292	0.97162	0.97178
DC60	0.04603	0.02983	0.03447
F1/2	0.00539	0.00184	0.00308
F2/2	0.00414	0.00827	0.00745
F3/2	0.00521	0.00479	0.00548
F4/2	0.00480	0.00258	0.00278
F5/2	0.00385	0.00520	0.00446
FM/2	0.00468	0.00454	0.00465

Table (5): Engine face performance CFD solutions for optimal micro-scale secondary flow control installation designs.

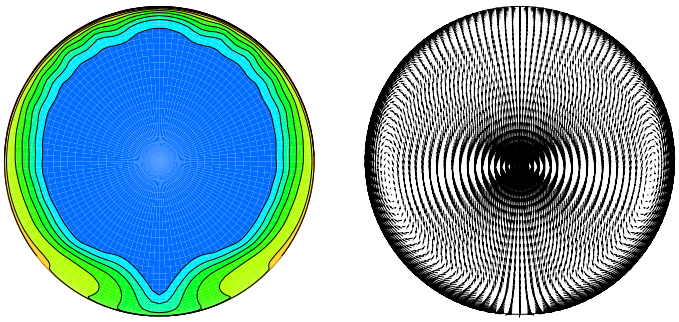

(a) Optimal “Maximum Performance” Solution

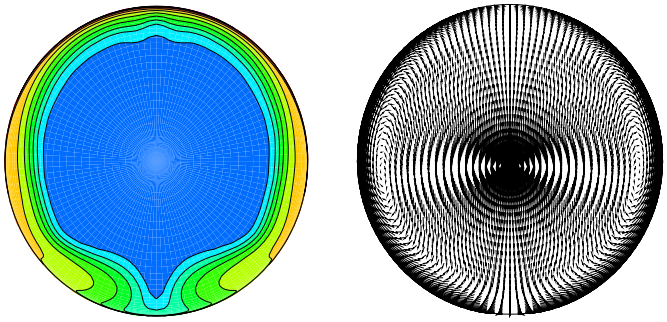

(b) Optimal “Maximum Engine Stability” Solution

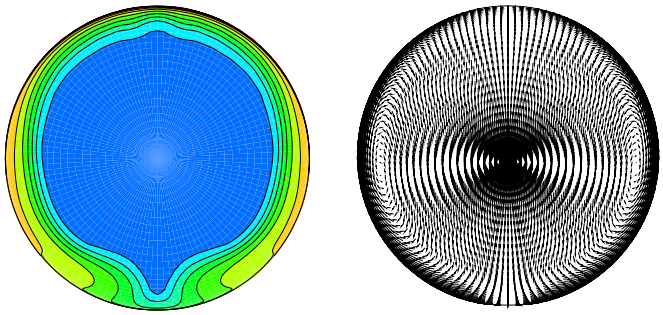

(c) Optimal “Maximum HCF Life Expectancy” Solution

Figure (9): Comparison of total pressure recovery contours for the optimal micro-scale secondary flow control installation CFD solutions.

The near wall streamlines for the baseline inlet solution and optimal Maximum HCF Life Expectancy installation design for a throat Mach number of 0.70 are shown in Figures (10) and (11). In the baseline flow presented in Figure (10), secondary motion or “over-turning” of the fluid, arises through an imbalance between centrifugal force and radial pressure gradient at wall of the first bend in the S-duct. This imbalance displaces high-speed fluid towards the outer (concave) wall and low-speed fluid towards the inner (convex) wall and leads to a generation of longitudinal vorticity which tend to congregate on the inner (convex) wall of the first bend. This forms the vortex pair in the inlet S-duct, which eventually “lifts-off”. See Figure (2). This vortex pair results in total pressure loss and severe total pressure distortion at the engine face.

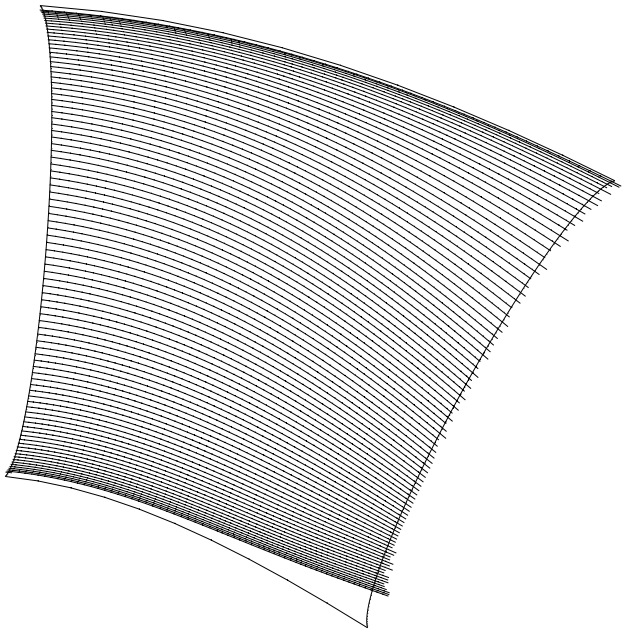

Figure (10): Baseline Inlet Solution

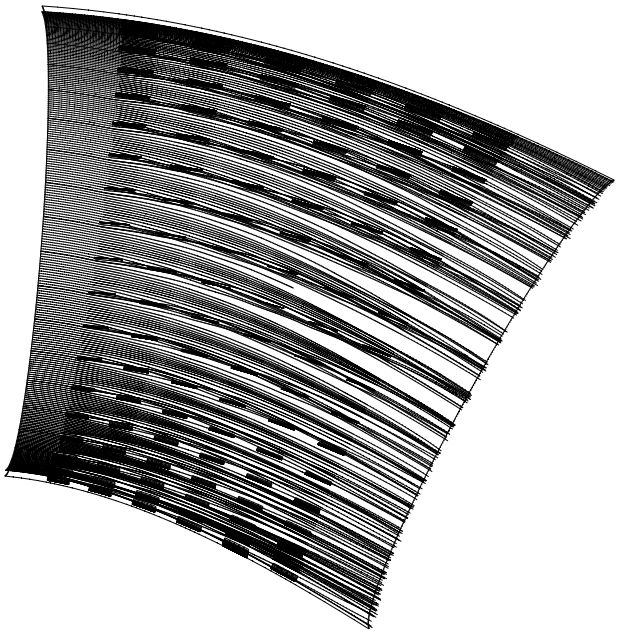

Figure (11): Optimal “Maximum HCF Life Expectancy” installation solution.

Notice the effect of the micro-vane actuators in preventing the over-turning of the flow adjacent to the inlet walls. This suppresses the formation of the passage vortex, thus resulting in the engine face distortion patterns displayed in Figure (9).

Comparison of the Optimal Installation Designs

Presented in Figure (12) is a comparison between the optimal pressure recovery performance for the single-band micro-vane installation designs, Figure (12a), and the multi-band micro-vane installation designs, Figure (12b). For the single-band and multi-band installation arrangement, the optimal Maximum Performance, Maximum Stability, and Maximum HCF Life Expectancy designs were compared with the baseline solution. For each band arrangement, micro-vane secondary flow control improved the pressure recovery performance in comparison to the baseline solution. However, there was substantially more total pressure recovery improvement for the single-band installation than for the multi-band concept. Thus, the greater number of discrete vortices induced by the multi-band arrangement generated higher losses relative to the single-band concept, although improvement over the baseline solution was still achieved.

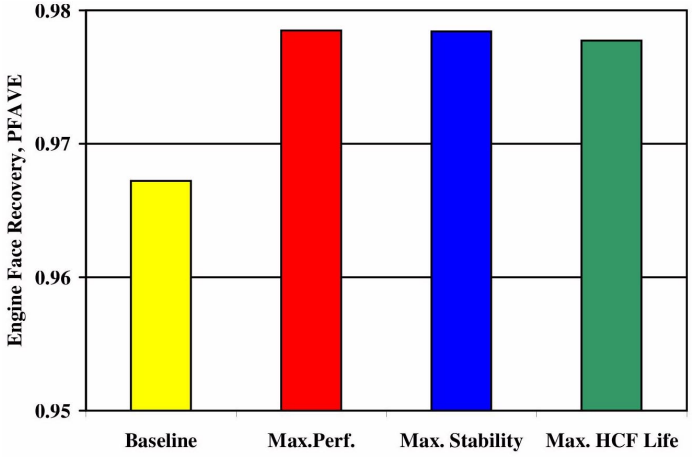

(a) Optimal Single Band Micro-Vane Installation Designs

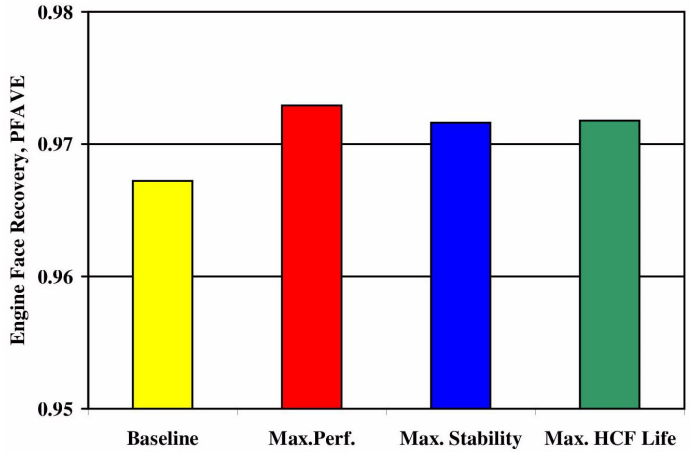

(b) Optimal Multi Band Micro-Vane Installation Designs

Figure (12): Effect of optimal micro-scale secondary flow installation designs on engine face total pressure recovery, (PFAVE).

Shown in Figure (13) is the effect of the optimal micro-scale secondary flow installation designs of engine face (DC60) distortion. Again for each band arrangement, the optimal Maximum Performance, Maximum Stability, and Maximum HCF Life Expectancy designs were compared with the baseline solution. In general, both the single-band and multi-band arrangement of micro-vane effectors substantially improved the inlet distortion characteristics over the baseline solution. See Figure (13a) and (13b). In addition, no strong conclusions can be reached as to the differences between the band arrangements with regards to managing engine face distortion.

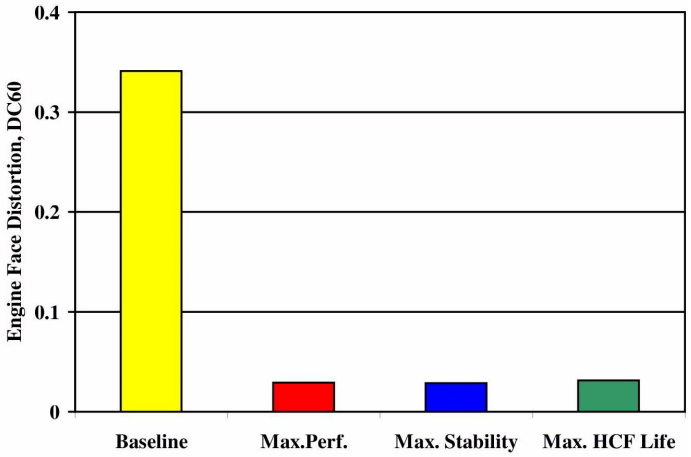

(a) Optimal Single Band Micro-Vane Installation Designs

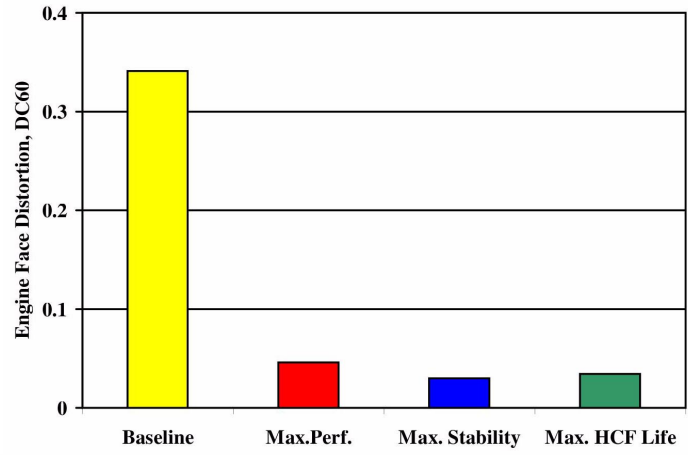

(b) Optimal Multi Band Micro-Vane Installation Designs

Figure (13): Effect of optimal micro-scale secondary flow installation designs on engine face distortion, (DC60).

Presented in Figure (14) is a comparison between the optimal harmonic 1/2 amplitude characteristics for the single-band micro-vane installation designs, Figure (14a), and the multi-band micro-vane installation designs, Figure (14b). In general, both the single-band and multi-band arrangement of micro-vane effectors substantially improved the first five Fourier harmonic 1/2 amplitude characteristics over the baseline solution. See Figure (14a) and (14b). In addition, no strong conclusions can be reached as to the differences between the band arrangements with regards to managing the first five Fourier harmonic 1/2 amplitudes of engine face distortion

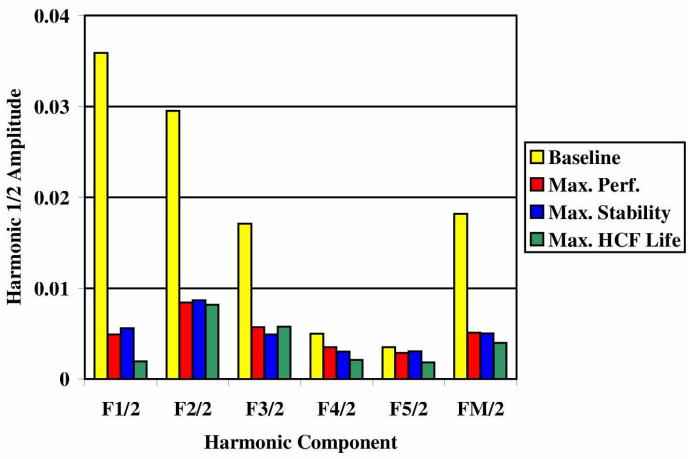

(a) Optimal Single Band Micro-Vane Installation Designs

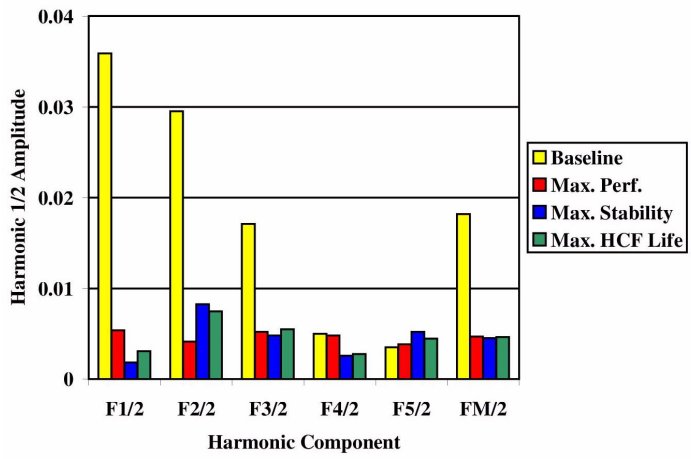

(b) Optimal Multi Band Micro-Vane Installation Designs

Figure (14): Effect of optimal micro-scale secondary flow installation designs on engine face Fourier harmonic 1/2 components of distortion, (Fi/2).

Comparison of CFD Analysis and DOE Prediction

Validation cases were included in this study and these are presented in Table (7), There are a total of three CFD validation cases. They represent the three "Optimal Robust" installation designs. The CFD validation performance results for "Optimal Robust" Maximum Performance, Maximum Engine Stability installation, and Maximum HCF Installation designs included all the response variables important for this study, i.e. inlet total pressure recovery (PFAVE), engine face distortion (DC60), and the first five Fourier harmonic 1/2-amplitudes of distortion (F1/2, F2/2, F3/2, F4/2, and F5/2). These results indicate that the three "Optimal Robust" installation designs satisfied the design requirements over the entire mission variable range. In order to validate the DOE performance prediction procedure, the three CFD performance validation cases were chosen for statistical comparison with the DOE predictions for all of the eight responce variables.

A direct statistical comparison can be made between the optimal responses predicted by the DOE models (Y_{DOE}) and the actual CFD predicted performance values (Y_{CFD}) through the expression:

$$t^* = \frac{\left|\ln(Y_{CFD}) - \ln(Y_{DOE})\right|}{\dfrac{\ln(Y_A) - \ln(Y_{DOE})}{t(0.975, N-p)}} \qquad (11)$$

where Y_A is the upper 95% confidence interval for the individual predicted response Y_{DOE} from the regression model, and t(0.975,N-p) is the 95% confidence t-value for N-p degrees of freedom.

When the span of the response data covers a decade or more, there often exist a functional relationship between the mean values and standard deviation of the data. Under these conditions, the data does not satisfy the requirement of a normally distributed set. Therefore, a transformation is often used to stabilize the variation over the response variable range. Because this was the case with DC60 and the Fourier harmonic 1/2-amplitudes, the natural logarithm of these responses were used in the DOE analysis and in this evaluation of the DOE regression model. Since all the response parameters except for PFAVE were analyzed using a natural log transformation, the natural log of the response (Y) was used in the statistical comparison of those response variables. For a statistically significant difference to exist between the DOE model predicted response (Y_{DOE}) and the CFD validation response prediction (Y_{CFD}), the expression:

$$t^* > t(0.975, N-p) \qquad (12)$$

must hold. Likewise, if the expression

$$t^* < t(0.975, N-p) \qquad (13)$$

is valid, the Y_{CFD} is not statistically different from Y_{DOE}. Therefore, for no significant statistical difference to exist between the DOE model predicted response Y_{DOE} and the CFD analysis response Y_{CFD}, the CFD response prediction must fall within the 95% confidence interval of the DOE model prediction for that response.

Table (7) shows the results of this statistical comparison at an inlet throat Mach Number of 0.70 and inlet angle-of-incidences of 0^o for the Maximum Performance, Maximum Engine Stability, and Maximum HCF Life Expectancy missions. In general, the number of incidences when the comparisons were statistically different was somewhat above 5%, which is remarkably good. All the cases in which a statistical difference were indicated involved in the evaluation of the Fourier harmonic 1/2-amplitudes of distortion. In these particular cases, the differences between the CFD analysis and DOE prediction were to too small to be of practical significance, i.e. there was no "meaningful statistical difference" This indicates that the DOE prediction results are not substantially different from the CFD analysis results (i.e. the CFD analysis predictions fell within the 95% confidence interval of the DOE performance predictions). It also indicates that the optimal installations determined by the DOE

models were a statistically valid optima when compared to the actual CFD installation analyses. The accuracy of the response surfaces determined from the DOE analysis was therefore more than adequate for use in determining an installation optimum.

Response	Mission	CFD	DOE	t	t*	Comments
PFAVE	Max. Perf.	0.97292	0.97358	2.26216	0.96721	Not Diff.
DC60		0.04603	0.05202	2.26216	0.32502	Not Diff.
F1/2		0.00539	0.00367	1.97681	0.76907	Not Diff.
F2/2		0.00414	0.00347	1.97681	0.31881	Not Diff.
F3/2		0.00521	0.00392	1.97669	2.07258	Diff.
F4/2		0.00480	0.00337	1.97669	0.80030	Not Diff.
F5/2		0.00385	0.00295	1.97669	0.81048	Not Diff.
FM/2		0.00468	0.00369	1.97681	0.84656	Not Diff.
PFAVE	Max. Stability	0.97126	0.97059	2.26216	1.07561	Not Diff.
DC60		0.02983	0.02936	2.26216	0.04364	Not Diff.
F1/2		0.00184	0.00197	1.97681	0.14992	Not Diff.
F2/2		0.00827	0.00479	1.97681	1.01101	Not Diff.
F3/2		0.00479	0.00398	1.97669	1.34175	Not Diff.
F4/2		0.00258	0.00269	1.97669	0.09433	Not Diff.
F5/2		0.00520	0.00368	1.97669	0.88621	Not Diff.
FM/2		0.00454	0.00319	1.97681	1.26802	Not Diff.
PFAVE	Max. HCF Life	0.97178	0.97178	2.26216	0.00636	Not Diff.
DC60		0.03447	0.03844	2.26216	0.30853	Not Diff.
F1/2		0.00308	0.00348	1.97681	0.26243	Not Diff.
F2/2		0.00745	0.00336	1.97681	1.47714	Not Diff.
F3/2		0.00548	0.00338	1.97669	3.55215	Diff.
F4/2		0.00278	0.00105	1.97669	2.28369	Diff.
F5/2		0.00446	0.00239	1.97669	1.61631	Not Diff.
FM/2		0.00465	0.00306	1.97681	1.49557	Not Diff.

Table (7): Statistical comparison between CFD analysis and DOE prediction for the optimal installation designs.

CONCLUSIONS

It is the purpose of this study to demonstrate the viability and economy of *Design-of-Experiments* (DOE) to arrive at micro-secondary flow control installation designs that achieve optimal inlet performance for different mission strategies. These statistical design concepts were used to investigate the properties of “low unit strength” micro-effector installation. “Low unit strength” micro-effectors are micro-vanes, set a very low angle-of-incidence, with very long chord lengths. They are designed to influence to near wall inlet flow over an extended streamwise distance. In this study, however, the long chord lengths were replicated by a series of short chord length effectors arranged in series over multiple bands of effectors. In order to properly evaluate the performances difference between the single band extended chord length installation designs and the segmented multi-band short chord length designs, both sets of installations must be optimal. Critical to achieving optimal micro-secondary flow control installation designs is the understanding of the factor interactions that occur between the multiple bands of micro-scale vane effectors. These factor interactions are best understood and brought together in an optimal manner through a structured Design-of-Experiments process, or more specifically *Response Surface Methods* (RSM).

To illustrate the potential of *Response Surface Methodology* to determine optimal micro-scale secondary flow installation designs, three different mission strategies were considered for the subject inlet, namely (1) Maximum Performance, (2) Maximum Engine Stability, and (3) Maximum High Cycle Fatigue Life Expectancy. The Maximum Performance mission minimized the inlet total pressure losses, the Maximum Engine Stability mission minimized the engine face distortion (DC60), while the Maximum HCF Life Expectancy mission minimized the mean of the first five Fourier harmonic amplitudes, i.e. “collectively” reduced all the harmonic 1/2-amplitudes of engine face distortion. Each of the mission strategies was subject to a low engine face distortion constraint, i.e. $DC60 < 0.10$, which is a level acceptable for commercial engines, and a constraint on each individual Fourier harmonic amplitude of $Fk/2 < 0.015$.

Comparison of the optimal single-band and multi-band installation design concepts for the Maximum Performance, Maximum Engine Stability, and Maximum High Cycle Fatigue Life Expectancy missions indicated that micro-scale flow controlled improved performance over the baseline solution. However, the multi-band installation concept had greater total pressure losses relative to the single-band arrangement. The larger number of individual vortices generated by the multi-band concept also generated greater losses. In comparing the optimal single-band and multi-band installation design concepts for the Maximum Performance, Maximum Engine Stability, and Maximum High Cycle Fatigue Life Expectancy missions relative to engine face DC60 distortion and the first five Fourier harmonic 1/2 amplitude of engine face distortion, no strong conclusions can be reached as to which arrangement is better. Therefore, the multi-band concept provided a viable concept for improving performance over the baseline performance. However, the penalty paid for the greater number of vortices generated by the multi-band arrangement were larger losses relative to the single-band design concept.

REFERENCES

(1) Anderson, B. H., Miller, D. M., Yagel, P. J, and Traux, P. P., “A Study of MEMS Flow Control for the Management of Engine Face Distortion in Compact Inlet Systems”, FEDSM99-6920, 3rd ASME/JSME Joint Fluids Engineering Conference, San Francisco, CA, July 18-23, 1999.

(2) Hamstra, J. W., Miller, D. N., Truax, P. P., Anderson, B. H., and Wendt, B. J., “Active Inlet Flow Control Technology Demonstration”, ICAS-2000-6.11.2, 22nd International Congress of the Aeronautical Sciences, Harrogate, UK, August 27th-September 1st, 2000.

(3) Anderson, B. H. and Keller, D. J., “Optimal Micro-Scale Secondary Flow Control for the Management of HCF and Distortion in Compact Inlet Diffusers”, NASA/TM-2002-211686, July 2002.

(4) Anderson, B. H. and Keller, D. J., “A Robust Design Methodology for Optimal Micro-Scale secondary Flow Control in Compact Inlet Diffusers”, AIAA Paper No. 2002-0541, Jan. 2002.

(5) Anderson, B. H. and Keller, D. J., “Robust Design Methodologies for Optimal Micro-Scale Secondary Flow Control in Compact Inlet Diffusers”, NASA/TM-2001-211477, March 2001.

(6) Anderson, B. H., Baust, Henry D., and Agrell, Johan: “Management of Total Pressure Recovery, Distortion, and High Cycle Fatigue in Compact Air Vehicle Inlets”, Proposed NASA TM, 2002.

(7) Anderson, B. H. and Keller, D. J., “Considerations in the Measurements of Engine Face Distortion for High Cycle Fatigue in Compact Inlet Diffusers”, NASA/M-2001-211476, March 2001.

(8) AGARD FTP Working Group 13, “Air Intakes for High Speed Vehicles”, AR-270, September 1991.

(9) Willmer, A. C., Brown, T. W. and Goldsmith, E. L., “Effects of Intake Geometry on Circular Pitot Intake Performance at Zero and Low Forward Speeds”, Aerodynamics of Power Plant Installation, AGARD CP301, Paper 5, Toulouse, France, May 1981, pp 51-56.

(10) Goldsmith, E. L. and Seddon, J. (eds), “Practical Intake Aerodynamics,” Blackwell Scientific Publications, Oxford, 1993.

(11) Bender, E. E, Anderson, B. H., and Yagle, P. J., “Vortex Generator Modeling for Navier Stokes Code”, FEDSM99-69219, 3rd ASME/JSME Joint Fluids Engineering Conference, San Francisco, CA, July 18-23, 1999.

REPORT DOCUMENTATION PAGE

Form Approved
OMB No. 0704-0188

1. AGENCY USE ONLY (*Leave blank*)	2. REPORT DATE	3. REPORT TYPE AND DATES COVERED
	January 2003	Technical Memorandum

4. TITLE AND SUBTITLE

Design-of-Experiments to Reduce Life-Cycle Costs in Combat Aircraft Inlets

5. FUNDING NUMBERS

WBS–22–708–92–21

6. AUTHOR(S)

Bernhard H. Anderson, Henry D. Baust, and Johan Agrell

7. PERFORMING ORGANIZATION NAME(S) AND ADDRESS(ES)

National Aeronautics and Space Administration
John H. Glenn Research Center at Lewis Field
Cleveland, Ohio 44135–3191

8. PERFORMING ORGANIZATION REPORT NUMBER

E–13720

9. SPONSORING/MONITORING AGENCY NAME(S) AND ADDRESS(ES)

National Aeronautics and Space Administration
Washington, DC 20546–0001

10. SPONSORING/MONITORING AGENCY REPORT NUMBER

NASA TM—2003-212017
AIAA–2003–0652

11. SUPPLEMENTARY NOTES

Prepared for the 41st Aerospace Sciences Meeting and Exhibit sponsored by the American Institute of Aeronautics and Astronautics, Reno, Nevada, January 6–9, 2003. Bernhard H. Anderson, NASA Glenn Research Center; Henry D. Baust, Wright Patterson Air Force Base, Dayton, Ohio 45433; Johan Agrell, Swedish Defence Research Agency, Bromma, Sweden. Responsible person, Bernhard H. Anderson, organization code 5850, 216–433–5822.

12a. DISTRIBUTION/AVAILABILITY STATEMENT

Unclassified - Unlimited
Subject Category: 07 Distribution: Nonstandard

Available electronically at http://gltrs.grc.nasa.gov

This publication is available from the NASA Center for AeroSpace Information, 301–621–0390.

12b. DISTRIBUTION CODE

13. ABSTRACT ***(Maximum 200 words)***

It is the purpose of this study to demonstrate the viability and economy of Design-of-Experiments (DOE), to arrive at micro-secondary flow control installation designs that achieve optimal inlet performance for different mission strategies. These statistical design concepts were used to investigate the properties of "low unit strength" micro-effector installation. "Low unit strength" micro-effectors are micro-vanes, set a very low angle-of incidence, with very long chord lengths. They are designed to influence the neat wall inlet flow over an extended streamwise distance. In this study, however, the long chord lengths were replicated by a series of short chord length effectors arranged in series over multiple bands of effectors. In order to properly evaluate the performance differences between the single band extended chord length installation designs and the segmented multiband short chord length designs, both sets of installations must be optimal. Critical to achieving optimal micro-secondary flow control installation designs is the understanding of the factor interactions that occur between the multiple bands of micro-scale vane effectors. These factor interactions are best understood and brought together in an optimal manner through a structured DOE process, or more specifically Response Surface Methods (RSM).

14. SUBJECT TERMS

Aerodynamics; Propulsion; Fluid dynamics

15. NUMBER OF PAGES

18

16. PRICE CODE

17. SECURITY CLASSIFICATION OF REPORT	18. SECURITY CLASSIFICATION OF THIS PAGE	19. SECURITY CLASSIFICATION OF ABSTRACT	20. LIMITATION OF ABSTRACT
Unclassified	Unclassified	Unclassified	